Characterization of a novel metabolic strategy used by drug-resistant tumor cells

MARY-ELLEN HARPER,* ANDREAS ANTONIOU,* ELIZABETH VILLALOBOS-MENUEY,† ALICIA RUSSO,‡ RICHARD TRAUGER,§ MINDA VENDEMELIO,§ AMANDA GEORGE,‡ RICHARD BARTHOLOMEW,§ DENNIS CARLO,§ AZHAR SHAIKH,* JAMI KUPPERMAN,‡ EVAN W. NEWELL,‖ IVAN A. BESPALOV,¶ SUSAN S. WALLACE,¶ YE LIU,# JEFFREY R. ROGERS,† GREGORY L. GIBBS,** JACK L. LEAHY,# ROBERT E. CAMLEY,†† ROBERT MELAMEDE,¶,† AND M. KAREN NEWELL†,1

*Department of Biochemistry, Microbiology and Immunology, Faculty of Medicine, University of Ottawa, Ottawa, Ontario, Canada; †Department of Biology, ††Department of Physics, University of Colorado at Colorado Springs, Colorado Springs, Colorado, USA; ‡Division of Immunobiology, #Division of Endocrinology, Department of Medicine, University of Vermont College of Medicine, Burlington, Vermont, USA; §Immune Response Corporation, San Diego, California, USA; ‖Toronto Western Research Institute and Department of Physiology, University of Toronto, Toronto, Ontario; ¶Department of Microbiology and Molecular Genetics, The Markey Center for Molecular Genetics, University of Vermont, Burlington, Vermont, USA; and **Colorado Associates in Medical Physics, Colorado Springs, Colorado, USA

ABSTRACT **Acquired or inherent drug resistance is the major problem in achieving successful cancer treatment. However, the mechanism(s) of pleiotropic drug resistance remains obscure. We have identified and characterized a cellular metabolic strategy that differentiates drug-resistant cells from drug-sensitive cells. This strategy may serve to protect drug-resistant cells from damage caused by chemotherapeutic agents and radiation. We show that drug-resistant cells have low mitochondrial membrane potential, use nonglucose carbon sources (fatty acids) for mitochondrial oxygen consumption when glucose becomes limited, and are protected from exogenous stress such as radiation. In addition, drug-resistant cells express high levels of mitochondrial uncoupling protein 2 (UCP2). The discovery of this metabolic strategy potentially facilitates the design of novel therapeutic approaches to drug resistance.—Harper, M.-E., Antoniou, A., Villalobos-Menuey, E., Russo, A., Trauger, R., Vendemelio, George, A. M., Bartholomew, R., Carlo, D., Shaikh, A., Kupperman, J., Newell, E. W., Bespalov, I. A., Wallace, S. S., Liu, Y., Rogers, J. R., Gibbs, G. L., Leahy, J. L., Camley, R. E., Melamede, R., Newell, M. K. Characterization of a novel metabolic strategy used by drug-resistant tumor cells. *FASEB J.* 16, 1550–1557 (2002)**

Key Words: cancer · mitochondria · uncoupling proteins · membrane potential · oxygen consumption

It is well known that drug-sensitive tumor cells, under the selective pressure of treatment with chemotherapeutic agents, develop into drug-resistant versions in many different tumor cells. In fact, drug resistance is the leading cause of death from cancer (1). Although some studies characterize features that distinguish drug-sensitive cells from drug-resistant cells (2), here we describe a novel metabolic mechanism that may enable tumor cells to survive many apoptosis-inducing stimuli. This mechanism allows us to classify the important characteristics of drug-sensitive tumor cells compared with drug-resistant tumor cells.

We will first review the basis of cellular energy metabolism because these processes are key to understanding the differences between the two cell types. In nondividing cells, mitochondria normally provide >90% of cellular ATP (3). The details of this energy storage process are complex, but there are key parameters that control ATP production. These include a proton gradient across the inner mitochondrial membrane, electron transport along the inner membrane, and respiratory complexes within the inner membrane (4). The membrane potential depends on the maintenance of a proton gradient across the inner mitochondrial membrane. Finally, we note that oxygen complexes are used to facilitate the electron flow. Thus, normal by-products of energy production are reactive oxygen intermediates (ROI) (5).

We have found that highly viable tumor cells generally fall into one of two categories. Cells associated with a sensitivity to chemotherapeutic agents and radiation are characterized by the following parameters when compared with drug-resistant cells:

1) Higher mitochondrial membrane potential;

2) The transfer of protons against the proton gradient of the mitochondria is larger;

3) Relatively low use of fat for fuel in the mitochon-

[1] Correspondence: Department of Biology, 134 Science Bldg., 1420 Austin Bluffs Pkwy., University of Colorado at Colorado Springs, Colorado Springs, CO 80918, USA. E-mail: mnewell@mail.uccs.edu

0892-6638/02/0016-1550 © FASEB

dria; production of ATP is primarily through use of glucose;

4) When stressed, they have higher levels of reactive oxygen;

5) In the normal, unstressed state they have lower DNA damage, when stressed, the DNA damage is increased;

6) In a stressed state the cells are susceptible to apoptosis.

Cells associated with a resistance to chemotherapeutic agents and radiation are characterized by a different set of parameters when compared with drug-sensitive cells:

1) Lower mitochondrial membrane potential;

2) The transfer of protons against the proton gradient of the mitochondria is smaller; there is a substantial proton 'leak';

3) Higher use of fat for fuel in the mitochondria accompanied by a higher rate of cytosolic glycolysis;

4) When stressed, they have lower levels of reactive oxygen;

5) In the normal, unstressed state they have higher DNA damage, but when stressed, the DNA damage is reduced;

6) In a stressed state, the cells are less susceptible to apoptosis.

We present evidence that it is precisely this set of differences between the two types of cells that results in a protective metabolic strategy for the drug- and radiation-insensitive cells.

It is interesting to compare the features described above to characteristics associated with uncoupling proteins. Uncoupling proteins are a family of molecules, first described in brown adipose tissue, that function as a metabolic switch (6, 7). These proteins have been shown to produce the following metabolic changes: dissipation of the proton gradient, lowering of mitochondrial membrane potential; induction of a metabolic shift to fatty acids as a source of fuel in mitochondria; promotion of high rates of glucose utilization in the cytosol and increased oxygen consumption in the mitochondria; and protection from reactive oxygen species (8). There is clearly a striking similarity between the known changes in metabolic activity produced by uncoupling proteins and the key features of drug resistance.

To test the idea that a metabolic shift can produce drug-resistant cells, we assessed the role of uncoupling protein 2 (UCP2) (9). We ask whether there is a significantly higher level of UCP2 in the mitochondria of drug-resistant cells. We concentrate on the presence of UCP2 in the mitochondria because the mitochondria is well established to be the cellular center for energy production. Our results show that UCP2 is expressed at higher levels in the mitochondria of drug-resistant cells, further supporting the connection between mitochondrial activity and cellular response to chemotherapeutic agents.

MATERIALS AND METHODS

Cell culture

All tumor cells were grown in culture in complete RPMI medium (supplemented with 5% fetal calf serum (FCS), glutamine, beta-mercapto-ethanol, sodium pyruvate, HEPES, antibiotics). Cell lines used in these studies include L1210 and L1210/DDP (10), HL60 (11), HL60.MDR (2), U937 (12), and B16.F1 (13) cells. L1210 is a mouse leukemia cell widely used as a model for testing drug sensitivity. L1210/DDP is a drug-resistant subline derived in cisplatin that exhibits dual resistance to methotrexate and cisplatin (10).

Confocal microscopy

Cells were harvested (1200 rpm, 10 min), counted, and resuspended at a concentration of 1×10^5 cells/mL; 450 μL of 1×10^5 cells/mL were added to a cytospin apparatus and spun on to microscope slides (600 rpm, 10 min). Slides were removed from cytospin apparatus, allowed to air dry, and placed in a coppin jar for fixation with methanol. Cells were treated with Mitotracker green (350 nm) and red (350 nm) for 30 min. As per manufacturer's instructions, cells were washed twice with permeabilization buffer, treated with one drop of Fluorosave, plated onto slides with coverslips, and sealed with clear nail polish. Confocal microscopy was performed using the Bio-Rad MRC 1024ES confocal microscope with laser excitations at 488 nM (blue excitation, green emission) and 568 (green excitation, red emission). The data were analyzed using Comos or LaserSharp software (Bio-Rad, Inc., Hercules, CA).

Studies of oxidative phosphorylation in intact cells

For simultaneous determinations of oxygen consumption and mitochondrial membrane potential, 1.0×10^7 cells/mL were incubated at a concentration in 106 mM NaCl, 0.41 mM $MgSO_4$, 25 mM $NaHCO_3$, 10 mM Na_2HPO_4, 10 mM glucose, 2.5 mM $CaCl_2$, and 5 mM KCl. Oxygen consumption rates were performed in duplicate using 1.0×10^7 cells at 37°C in a Hansatech (Norfolk, U.K.) Clark-type oxygen electrode. Mitochondrial membrane potentials were calculated based on the distribution of $[^3H]$-H_2O, $[^{14}C]$methoxyinulin, and $[^3H]$ methyltriphenylphosphonium cation (TPMP+) as described by Nobes et al. (14) and Harper and Brand (15).

For simultaneous determinations of oxygen consumption and mitochondrial membrane potential, cells were incubated at a concentration of 1.0×10^7 cells/mL in (mM) 106 NaCl, 0.41 $MgSO_4$, 25 $NaHCO_3$, 10 Na_2HPO_4, 10 glucose, 2.5 $CaCl_2$, and 5 KCl. Cells were preincubated at 37°C for 10 min to allow the cells to establish steady-state ion gradients. Various inhibitors and/or isotopes were added to the vials and the incubation period continued for an additional 20 min. Saturating concentrations of oligomycin (100 nM) were added to produce state 4 (i.e., nonphosphorylating) respiration conditions. To characterize the responsiveness of mitochondrial proton leak reactions to decreasing mitochondrial membrane potential ($\Delta\Psi_m$), incremental amounts of the electron transport chain inhibitor antimycin were added (50 nM, 250 nM, and 5 μM). To characterize the responsiveness of the ATP synthesis and turnover reactions in cells incubated in the absence of oligomycin, increasing amounts of antimycin were added (100 and 200 nM).

Oxygen consumption

For each cell preparation, assessments were performed in duplicate, using 1.0×10^7 cells at 37°C in a Hansatech (Norfolk, U.K.) Clark-type oxygen electrode.

Mitochondrial membrane potential

Mitochondrial membrane potential ($\Delta\Psi_m$) was calculated based on the distribution of [^{3}H]-H_2O, [^{14}C]methoxyinulin, and [^{3}H] methyltriphenylphosphonium cation as described by Nobes et al. (14) and Harper and Brand (16). For each cell preparation, assessments were performed in triplicate. $\Delta\Psi_m$ is calculated by knowing the proportion of cytoplasmic volume occupied by the mitochondrial matrix [(V_m/V_c) or mitochondrial volume/cell volume], the apparent activity coefficient of $TPMP^+$ in the extracellular, cytoplasmic plus nuclear, and mitochondrial compartments (a_e, a_c, and a_m, respectively), and the extent of $TPMP^+$ accumulation into the whole cell ($[TPMP^+]_t/[TPMP^+]_c$) and cytoplasm in relation to the external medium ($[Cl^-]_c/[Cl^-]_t$), where t = total and e = extracellular. The apparent volume of pellet available to each isotope, measured as its space in mL, was calculated as dpm in total pellet divided by dpm/mL of supernatant sample. The [^{3}H]$TPMP^+$ accumulation ratio ($[TPMP^+]_t/[TPMP^+]_c$) was calculated as ([^{3}H]$TPMP^+$-[^{14}C]methoxyinulin)/(^3H_2O-[^{14}C]methoxyinulin).

Rates of glucose utilization and oxidation

Rates of glucose utilization were measured by the method of Ashcroft et al. Cells were incubated 90 min at 37°C in 100 μL KRB, glucose (5.5 mM), 1.3 μCi D-[5-^{3}H] glucose (Amersham, Arlington Heights, IL). The reaction was carried out in a 1 mL cup contained in a rubber-stoppered 20 mL scintillation vial that had 500 μL of distilled water surrounding the cup. Glucose metabolism was stopped by injecting 100 μL 1 M HCl through the stopper into the cup. An overnight incubation at 37°C was carried out to allow equilibration of the [^{3}H]-H_2O in the reaction cup and the distilled water, followed by liquid scintillation counting of the distilled water. Rates of mitochondrial glucose oxidation were measured by incubating cells for 90 min at 37°C in 100 μL of reaction buffer, glucose (2.8, 8.3, 27.7 mmol/L), 1.7 mCi 14C glucose. The reaction was carried out in a 1 mL cup in a 20 mL scintillation vial capped by a rubber stopper with a center well containing filter paper. Metabolism was stopped and CO_2 liberated with 300 μL 1 mol/L HCl injected through the stopper into the cup containing the cells. CO_2 was trapped in the filter paper by injecting 10 mL 1 mol/L KOH into the center well, followed 2 h later by liquid scintillation counting. Tubes containing $NaHCO_3$ and no cells were used to estimate the recovery of $^{14}CO_2$ in the filter paper, routinely close to 100%.

Rates of oleic acid oxidation

Rates of oleate consumption were measured by incubating cells for 90 min at 37°C in 100 mL of reaction buffer, oleic acid, and increasing concentrations of glucose (2.8, 8.3, 27.7 mmol/L), 1.7 mCi [U-^{14}C oleic acid], and cold oleate. The reaction was carried out in a 1 mL cup in a 20 mL scintillation vial capped by a rubber stopper with a center well that contained filter paper. Metabolism was stopped and CO_2 liberated with 300 mL 1 mol/L HCl injected through the stopper into the cup containing the cells. CO_2 was trapped in the filter paper by injecting 10 mL 1 mol/L KOH into the center well, followed 2 h later by liquid scintillation counting. Tubes containing $NaHCO_3$ and no cells were used to estimate the recovery of $^{14}CO_2$ in the filter paper, routinely close to 100%.

Quantitation of intracellular ATP levels

For each determination, 50,000 cells were harvested and washed twice in phosphate-buffered saline (PBS). Cells were lysed by boiling for 1 min in 300 μL of a glycine buffer (20 mM glycine, 50 mM $MgSO_4$, 4 mM EDTA, pH 7.4) and lysates were stored at −20°C. This allowed for duplicate determinations; however, for each experiment the ATP content of each cell type was determined from 6 separate aliquots of cells. Luciferase-luciferin reagent (0.5 mg/mL; Sigma L0633) was used to assay ATP content. Data were obtained from a liquid scintillation counter. A standard curve for ATP (50–700 nM in 50 nM increments) was constructed.

Flow cytometry

Cells were harvested, counted, and resuspended at 10^6 cells/100 μL in preparation for flow cytometric analysis. For DNA staining, cells were washed and resuspended in ice-cold PBS, then fixed by the dropwise addition of 95% ethanol. Cells were incubated for 30 min on ice, washed, and resuspended in PBS containing 1% formaldehyde and 0.01% Tween. The cells were then incubated with the anti DNA Fab (166, kind gift of Dr. Susan Wallace, University of Vermont), washed, and stained with a fluorescein-conjugated second-step anti-mouse immunoglobulin. Cells were washed and resuspended in PBS/3% BSA/1% formaldehyde. Cells were stained for intracellular H_20_2 using 6-carboxy-2′,7′-dichlorodihydrofluorescein diacetate (DCF-DA, Molecular Probes, Eugene, OR). Cells were incubated with 1 mM DCF-DA for 20 min, washed twice in PBS containing 5% FCS, and analyzed flow cytometrically. Mitochondrial membrane potential was assessed using Mitotracker red (CM-H_2XROS, Molecular Probes, Eugene, OR). The cells were resuspended in warm (37°C) PBS containing a final concentration of 0.5 micromolar dye. The cells were incubated for 30 min, pelleted, and resuspended in prewarmed medium for analysis. Data were acquired on a Coulter Elite Epics or Excel flow cytometer (Coulter, Hialeah, FL) and analyzed with CellQuest software, (Becton Dickinson, San Jose, CA). The Coulter Epics Elite flow cytometer has a single excitation wavelength (488 nm) and band filters for PE (575 nm), FITC (525 nm), and red (613 nm) that was used to analyze the stained cells. Each sample population was classified for cell size (forward scatter) and complexity (side scatter), gated on a population of interest and evaluated using 40,000 cells. Each figure describing flow cytometric data represents one of at least four replicate experiments.

Measurement of cytochrome *c* oxidase activity

Cytochrome *c* oxidase activity was determined in cellular homogenates using a spectrophotometric assay. This assay measures the rate at which cytochrome oxidase can oxidize its substrate, cytochrome *c*. This is done be measuring the rate of disappearance of the reduced cytochrome *c*, which absorbs light at 550 nm. Cellular homogenates were treated with 0.3% Lubrol WX (1 mM Lubrol/10 mg protein), diluted in 100 mM phosphate buffer (pH 7.0) to a final protein concentration of 1.0 mg/mL, and kept on ice for 1.5 h. During this time, a 200 mM cytochrome *c* solution was prepared containing 10% ascorbic acid. For each determination, an aliquot of diluted cellular homogenate (100 mg) was added to the cytochrome *c* solution and the absorbance was measured immediately for 1 min at 550 nm. Six different cytochrome *c* concentrations were used to construct a Lineweaver-Burk plot for the determination of V_{max}.

Statistical analysis

Data were expressed as mean ± SE and analyzed by unpaired *t* tests using Prism 2.0 for Windows. *P* values of <0.05 were considered significant.

Mitochondrial isolation and Western blot analysis

Mitochondria were isolated using differential centrifugation as adapted from ref 17. Cell homogenates were centrifuged at 1000 *g* for 10 min. The supernatants were then centrifuged at 12,000 *g* for 10 min to obtain the mitochondrial fractions. Mitochondria were resuspended in isolation medium and centrifuged again at 12,000 *g* for 10 min, and resuspended in (mM) 120 KCl, 20 sucrose, 20 glucose, 10 KH_2PO_4, 5 HEPES, 2 $MgCl_2$, and 1 EGTA. For Western blotting, 60 mg of mitochondrial protein was used in each lane. The primary antibody was goat anti-human UCP2 (1.5 μg/mL) (Santa Cruz Biotechnology, Santa Cruz, CA). The secondary antibody was anti-goat IgG-HRP (Santa Cruz Biotechnology) at 1:5,000. Chemiluminescent detection: Amersham ECL kit.

RESULTS AND DISCUSSION

As discussed, we wanted to determine the differences in metabolic characteristics between drug-resistant and -sensitive cells. We compared characteristics of mitochondrial metabolism in drug-sensitive and drug-resistant cells (18) by staining representative cell lines with the mitochondrial dyes Mitotracker green, which quantitates mitochondria, and CmCX Ros Mitotracker red (Molecular Probes, Eugene, OR), which reflects mitochondrial membrane potential. In **Fig. 1**, we see that the intensity for cells stained with Mitotracker green is approximately the same for all cell lines, suggesting that the numbers of mitochondria per cell are approximately the same. In contrast, the intensity of the cells stained with Mitotracker red differs between cell lines. The intensity is distinctly lower for the drug-resistant cells L1210/DDP and HL60.MDR and the inherently resistant melanoma B16.F1. This indicates that the resistant cell lines consistently have a lower mitochondrial membrane potential.

We note that HL60.MDR cells overexpress the multidrug resistance gene P-glycoprotein 1, which serves as a drug antiporter. Several studies suggest that P-gp 1-overexpressing cells can actively 'pump out' mitochondrial dyes (19). Therefore, it is possible that membrane potential measurements in HL60.MDR cells underestimate the true membrane potential because the dye may be pumped out. Thus, it is appropriate to confirm these results using alternative measurements of mitochondrial membrane potential. There is another reason to quantitate membrane potential in both cell lines, as differences in fluorescence could be a function of different numbers of mitochondria per cell.

To address these issues, we conducted a full analysis of the overall metabolic kinetics of oxidative phosphorylation using L1210 and L1210/DDP cells and HL60 and HL60.MDR cells as models of drug-sensitive and drug-resistant cells, respectively. The results are expressed as the overall kinetics of mitochondrial proton leak reactions (**Fig. 2**). These analyses require simultaneous dual determinations of membrane potential and oxygen consumption and the use of specific mitochondrial inhibitors (see Materials and Methods). State 4 oxygen consumption and membrane potential values

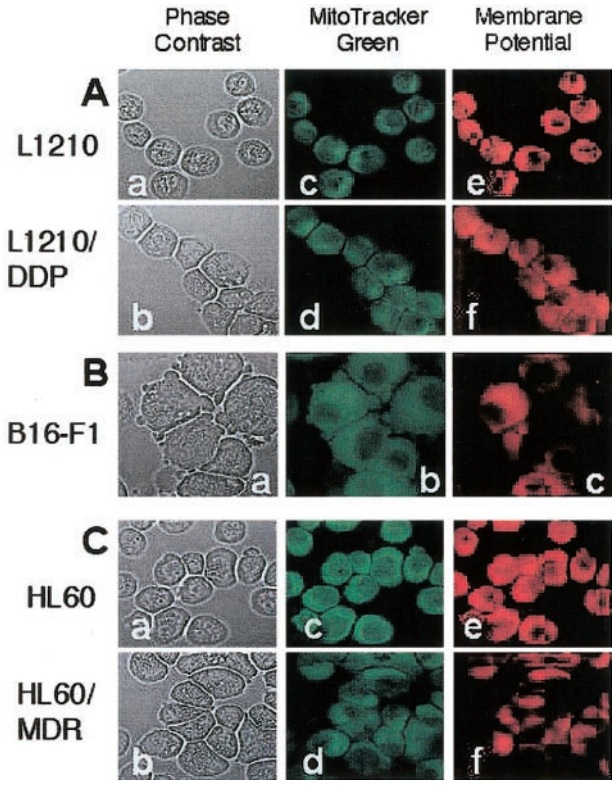

Figure 1. Confocal images of drug-sensitive and drug-resistant tumor cells, mitochondria, and mitochondrial membrane potential. Drug-sensitive L1210, a drug-resistant subline L1210/DDP (upper panel), inherently resistant melanoma B16.F1 (middle panel), drug-sensitive HL60, and drug-resistant HL60.MDR (lower panel) were examined. Whereas numbers of mitochondria are similar, as indicated by intensity of green in the middle panel, the membrane potential is lower in the drug-resistant (L1210/DDP) and inherently resistant (B16.F1 melanoma) cells, as indicated by lower intensity of red.

in the L1210/DDP and the HL60. MDR cells are clearly consistent with uncoupled mitochondrial respiration by these analyses. Mitochondrial membrane potential, as determined by the quantitative method employing the lipophilic cation, $TPMP^+$, is dramatically lower in the resistant sublines of cells. The overall kinetics of proton leak reactions are shown in the curved line extending to the left of state 4 values. Leak dependent oxygen consumption for a given value of mitochondrial membrane potential (e.g., between 145 and 150 mV) is markedly higher in the L1210/DDP and HL60.MDR cells than in the drug-sensitive cells. Thus, proton leak appears to be increased in the resistant cell types. The overall kinetics of substrate oxidation (represented by the line connecting state 4 and resting points) and of phosphorylation (represented by the line extending from the left of the resting value) are quite different in drug-sensitive (L1210 and HL60) and -resistant (L1210/DDP and HL60.MDR) cell lines. These quantitative results confirm the qualitative confocal microscopic results from Fig. 1 that show lower mitochondrial membrane potential in the drug-resistant cells.

As discussed above, there is a possibility that drug-

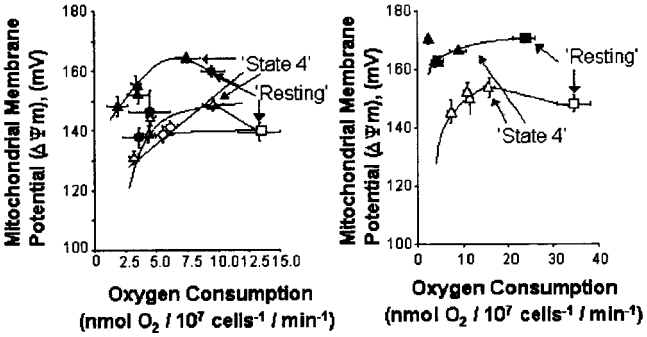

Figure 2. Mitochondrial membrane potential is lower and oxidative phosphorylation is uncoupled in drug-resistant cells vs. drug-sensitive cells. Filled symbols: L1210 cells (drug-sensitive); open symbols: L1210/DDP (drug-resistant) cells, left panel; filled symbols: HL60 (drug-sensitive) and open symbols: HL60.MDR (drug-resistant), right panel. Oxygen consumption and mitochondrial membrane potential were assessed simultaneously in the absence ('resting') and presence of mitochondrial inhibitors (antimycin and oligomycin, triangles; antimycin alone, circles) to examine the responsiveness of oxidative phosphorylation reactions under various metabolic conditions as described in Materials and Methods.

sensitive and -resistant cells have different numbers of mitochondria per cell. To address this issue, we measured activity of cytochrome *c* oxidase, a widely accepted indicator of mitochondrial mass (**Table 1**). The results demonstrate that total cellular mitochondrial content is higher in the drug-resistant sublines. Because oxygen consumption occurs only in the mitochondria, it is appropriate to normalize cellular oxygen consumption by dividing by the mitochondrial mass. When we do this, we find that the oxygen consumption per mitochondria in drug-resistant cells is relatively low compared with drug-sensitive cells. Taken together, the results indicate a significant difference in metabolism between the drug-resistant and drug-sensitive cells. This is particularly evident in the rates of oxygen consumption per mitochondria. We conclude that an individual mitochondria in the resistant cell is playing a different metabolic role than its counterpart in the sensitive cell.

Because we have argued that the mitochondria function differently in the sensitive and resistant cell lines, it is reasonable to ask how fuel is used in different kinds of cells. For example, in the well-characterized brown adipocyte, which changes from high to low mitochondrial membrane potential, there is an accompanying shift in fuel source from glucose to fatty acids (20). Reasoning that drug-resistant cells might behave similarly, we determined experimentally that under conditions of limiting glucose, the drug-resistant cells more readily use oleic acid as a carbon source compared with the drug-sensitive cells (**Fig. 3**). The data suggest that resistant cells with low mitochondrial membrane potential (as in active brown adipocytes), but not the drug-sensitive tumor cells, have the ability to shift to the oxidation of fatty acids when glucose supplies are limiting.

Because a substantial membrane potential is required for mitochondrial ATP synthesis and since we have seen a clear difference in membrane potential between drug-sensitive and drug-resistant cells, we compared levels of ATP between sensitive and resistant cells (**Table 2**). ATP was assayed on a per cell basis with corrections for differences in total protein content between the drug-sensitive and -resistant cell lines. The results show that levels of ATP (when normalized by mitochondrial mass or by protein mass) are lower in the drug-resistant cells. On the other hand, the total ATP content per cell is higher in the drug-resistant

TABLE 1. *Assessment of cytochrome oxidase activity and oxygen consumption*

Cytochrome oxidase activity (nmol cytochrome *c* oxidized/min/10^3 cells)				
Cell line	L1210	L1210/DDP	HL60	HL60.MDR
Mean	21.27	82.05	12.48	38.00
SE	3.74	8.24	2.14	4.56
*n**	3	3	4	4

Oxygen consumption (normalized to mitochondrial content, cytochrome activity)						
	State 4 O_2 consumed			Total cellular O_2 consumed		
Cell line	Mean	(SE)	*n**	Mean	(SE)	*n**
L1210	35.01	(3.91)	8	44.54	(4.03)	7
L1210/DDP	11.72	(0.93)	8	16.24	(1.96)	8
HL60	72.11	(13.92)	6	190.00	(19.40)	6
HL60.MDR	41.44	(2.89)	7	91.43	(91.43)	7

* *n* = Number of separate cell preparations studied; the assay was conducted in triplicate for each cell preparation.

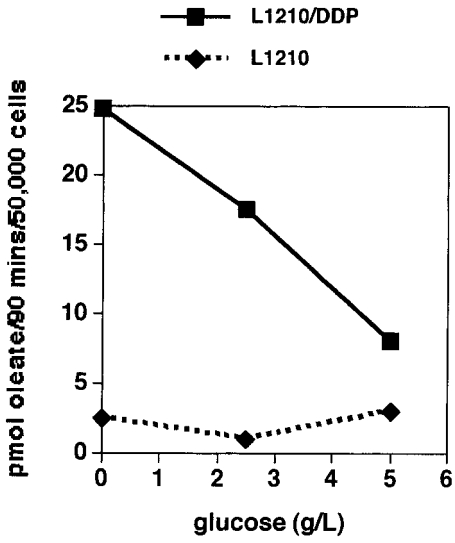

Figure 3. Drug-resistant cells preferentially use oleic acid as a mitochondrial carbon source when glucose levels drop. Rates of oleic acid oxidation were measured by incubating drug-sensitive cells L1210 (circles) or drug-resistant cells L1210/DDP (squares) with increasing (14) C oleic acid concentrations of glucose (2.8, 8.3, 27.7 mmol/L), as described in Materials and Methods.

TABLE 2. *Quantitation of intracellular ATP*[a]

ATP content (pmol/μg cellular protein)*		
Cell line	L1210	L1210/DDP
Mean	9.0560	5.050
SE	0.4965	0.325
*n**	3	3
ATP content (pmol/μmol cytochrome *c* oxidase)†		
Cell line	L1210	L1210/DDP
Mean	59.24	26.32
SE	3.245	1.695
*n**	3	3

*n** = Number of separate cell preparations studied; for each cell preparation the assay was conducted in triplicate. * $P = 0.0009$; † $P = 0.0002$.

cells. This suggests that synthesis of ATP by an individual mitochondria in the drug-resistant cells is inefficient. The numbers in Table 2 provide only an upper limit for the amount of ATP that can be produced per mitochondria. An additional source of ATP for the drug-resistant cells could be provided by a high rate of glycolysis. We have in fact confirmed this for several cell lines, as shown in **Table 3**.

The paradoxical shift from efficient respiration to highly inefficient, high-rate glycolysis to produce ATP has been proposed as a mechanism to protect newly synthesized and exposed DNA that could be damaged by reactive oxygen species. Using flow cytometry, we measured H_2O_2 production before and after gamma ray irradiation in L1210, L1210/DDP, HL60, and HL60.MDR cells. The results are presented in **Fig. 4**. The choice of H_20_2 is based on the fact that this is a common intermediate and has a lifetime long enough to measure. The key results shown are that radiation increases levels of reactive oxygen in drug-sensitive cells, but in drug-resistant cells radiation produces a decrease or minimal change in reactive oxygen levels.

To directly test the effect of reactive oxygen intermediates on DNA damage, we stained L1210 and L1210/DDP cells using an antibody (Fab 166) to the DNA

TABLE 3. *Glucose metabolism in L1210/0 and L1210/DDP and (inherently resistant) B16.F1 tumor cell lines*

	L1210/0	L1210/DDP	B16.F1 melanoma
Glucose utilization (pmol glucose/ 90 min/50,000 cells)	1740 ± 920	3470 ± 460	1500 ± 600
Glucose oxidation (pmol glucose/ 90 min/50,000 cells)	235 ± 7	428 ± 124	270 ± 70
Glucose utilization/oxidation	7.4	8.1	5.5

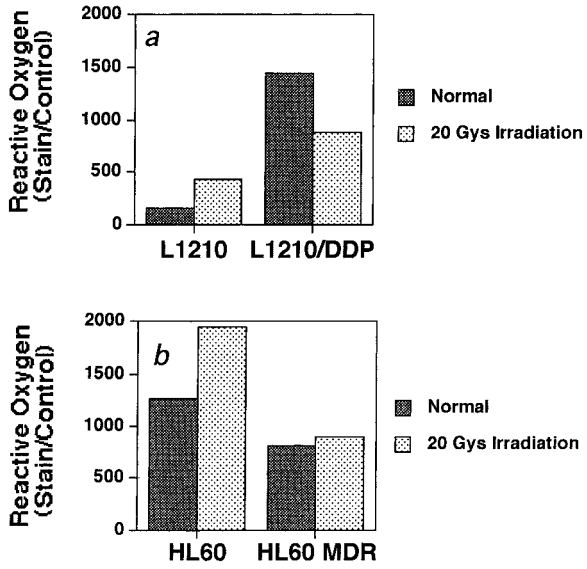

Figure 4. Radiation results in greater increases in H_20_2 in drug-sensitive cells vs. drug-resistant cells. *a)* Levels of hydrogen peroxide in untreated (light bars) vs. irradiated (20 grays) (dark bars) L1210 cells and L1210/DDP; *b)* levels of hydrogen peroxide in untreated (light bars) and irradiated (dark bars) HL60 and HL60.MDR cells, lower panel.

adduct 8-oxo-guanine (21). This antibody detects adducts of DNA that have become oxidized in the presence of molecular oxygen intermediates. We found a positive correlation between the presence of reactive oxygen and the detection of damage as measured by increased levels of 8-oxoguanine (**Fig. 5**). The drug-sensitive cells clearly show an increase in damage after irradiation. In contrast, the drug-resistant cells show a minimal increase in damage after irradiation. There are several possibilities to explain this result. One is that drug-resistant cells are better at repairing damage induced by stress. A different explanation is that drug-resistant cells are protected from additional stress-induced damage.

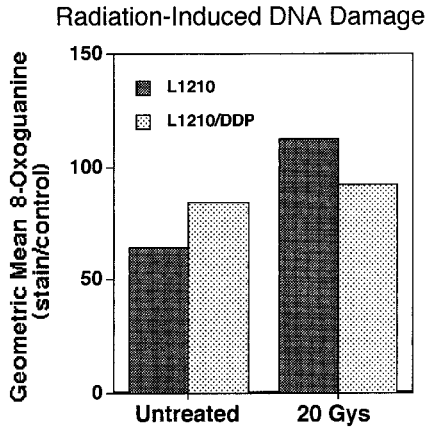

Figure 5. Radiation results in greater increases in DNA damage in L1210 than in L1210 DDP. DNA damage was detected flow cytometrically using an antibody to 8-oxoguanine in untreated (light bars) and irradiated (20 grays, gray line; dark bars). This represents 1 of at least 10 experiments with similar results.

Throughout this work we have connected differences in metabolic behavior with differences in sensitivity to drugs. The results above are all consistent with the idea that a metabolic shift can produce drug-resistant cells. We reasoned that one possible mechanism accounting for lower mitochondrial membrane potential in the drug-resistant cells could be through the activity of the UCP2 (7). We measured the presence of UCP2 in mitochondria of these cells by isolating mitochondria and using antibodies to UCP2 in Western blot analysis (**Fig. 6**). The results demonstrate that the drug-sensitive cells (L1210) and the resistant cell lines (L1210/DDP) both express mitochondrial UCP2. Significantly higher levels of UCP2 were detected consistently in all of the resistant cell lines (data not shown). This result correlates with measurements of lower mitochondrial membrane potential in the resistant cell lines, suggesting that UCP2 may be involved in lowering membrane potential.

The metabolic mechanism described here appears to be widely used in multiple drug-resistant phenotypes in tumor cells derived from a wide variety of tissue origins. Inherently resistant tumor cells such as melanoma exhibit the phenotype without selection in drugs. We propose that this metabolic strategy provides the basis for survival of inherently resistant or drug-selected resistant cells and accounts for the commonly recognized dual resistance to both drugs and irradiation. We suggest that the decrease in the rate of respiration accompanied by the highly increased rate of cytosolic glycolysis widely observed in drug-resistant cells mimics the protective strategy of seeds or spores, i.e., seeds and spores can remain relatively inert under conditions of limiting nutrients or adverse conditions. This is illustrated by the data in Fig. 4 showing that when glucose becomes limiting, resistant cells use fatty acids. In the case of the drug-resistant tumor cells, the adverse conditions are provided by the chemotherapeutic agents or radiation used to treat the tumor.

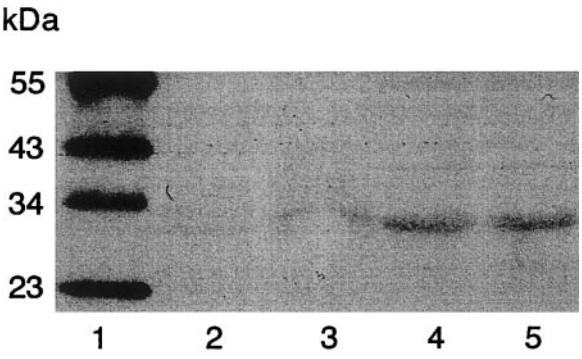

Figure 6. Representative Western blot of protein isolated from purified mitochondrial fractions of L1210 and L1210/DDP cells. Mitochondria were isolated using differential centrifugation as adapted from Reinhart et al. (17). Lane 1: Molecular weight markers (Santa Cruz). Lanes 2, 3: L1210 mitochondrial protein (50 mg) from two distinct mitochondrial preparations. Lanes 4, 5: L1210/DDP mitochondrial protein (50 mg) from two distinct mitochondrial preparations. Goat anti-human UCP2 (1.5 μg/mL). The secondary antibody was anti-goat IgG-HRP (Santa Cruz Bio/Technology) at 1:5,000. Chemiluminescent detection: Amersham ECL kit (Amersham).

The discovery of this metabolic approach in drug-resistant tumor cells affects tumor therapeutics and potentially the therapeutic approach to other diseases where free radical damage is involved. For example, it is known that the proton dissipating activity of uncoupling proteins can be turned off by nucleotides such as ATP. Therefore, if we can selectively target nucleotides to inhibit the metabolic strategy of the drug-resistant tumor cells, we may be able to reduce or eliminate the associated drug resistance. FJ

M.K.N. was supported by the Immune Response Corporation and grants from the National Institutes of Health (NIH) (RO1 GM62562 and RO1 HL61346). M.E.H. was supported by Natural Sciences and Engineering Research Council of Canada. J.L. was supported by NIH grant DK 56818. S.W. was supported by a grant from the Department of Energy.

REFERENCES

1. Landowski, T. H., Gleason-Guzman, M. C., and Dalton, M. S. (1997) Selection for drug resistance results in resistance to Fas-mediated apoptosis. *Blood* **89,** 1854–1861
2. Yu, D. S., Chang, S. Y., and Ma, C. P. (1997) The correlation of membranous glycoprotein-gp-170, cytoplasmic glutathione and glucose-6-phosphate dehydrogenase levels with multidrug resistance in transitional cell carcinoma cell lines of the urinary tract. *J. Urol.* **157,** 727–731
3. Rolfe, D. F. S., and Brown, G. C. (1997) Cellular energy utilization and molecular origin of standard metabolic rate in mammals. *Phys. Rev.* **77,** 731–758
4. Brand, M. D. (1990) The proton leak across the mitochondria inner membrane. *Biochim. Biophys. Acta* **1018,** 128–133
5. Garcia-Ruiz, C., Colell, A., Morales, A., Kaplowitz, N., and Fernandez-Checa, J. C. (1995) Role of oxidative stress generated from the mitochondrial electron transport chain and mitochondrial glutathione status in loss of mitochondrial function and activation of transcription factor nuclear factor-kappa B: studies with isolated mitochondria and rat hepatocytes. *Mol. Pharmacol.* **48,** 825–834
6. Boss, O., Muzzin, P., and Giacobino, J.-P. (1998) The uncoupling proteins–a review. *Eur. J. Endocrinol.* **139,** 1–9
7. Ricquier, D., and Bouillaud, F. (2000) The uncoupling protein homologues: UCP1, UCP2, UCP3, StUCP, and AtUCP. *Biochem. J.* **345,** 161–179
8. Negre-Salvayre, A., Hirtz, C., Carrera, G., Cazenave, R., Troly, M., Salvayre, R., Penicaud, L., and Casteilla, L. (1997) A role for uncoupling protein- 2 as a regulator of mitochondrial hydrogen peroxide generation. *FASEB J.* **11,** 809–815
9. Fleury, C., Neverova, M., Collins, S., Raimbault, S., Champigny, O., Levi-Meyrueis, C., Bouillaud, F., Seldin, M. F., Surwit, R. S., Ricquier, D,, and Warden, C. H. (1997) Uncoupling protein- **2,** a novel gene linked to obesity and hyperinsulinemia. *Nature Genet.* **15,** 269–272
10. Bhushan, A., Wroblewski, D., Xuan, Y., Tritton, T. R., and Hacker, M. P. (1996) Correlation of altered tyrosine phosphorylation with methotrexate resistance in a cisplatin-resistant subline of L1210 cells. *Biochem. Pharmacol.* **51,** 477–482
11. Macfarlane, D. E. (1986) Phorbol diester-induced phosphorylation of nuclear matrix proteins in HL60 promyelocytes. *J. Biol. Chem.* **261,** 6947–6953
12. Halicka, H. D., Ardelt, B., Li, X., Melamed, M. M., and Darzynkiewicz, Z. (1995) 2-Deoxy-D-glucose enhances sensitivity of human histiocytic lymphoma U937 cells to apoptosis induced by tumor necrosis factor. *Cancer Res.* **55,** 444–449
13. Townsend, S., and Allison, J. (1993) Tumor rejection after direct costimulation of CD8+ T cells by B7-transfected melanoma cells. *Science* **259,** 368–370

14. Nobes, C. D., Brown, G. C., Olive, P. N., and Brand, M. D. (1990) Non-ohmic conductance of the mitochondrial inner membrane in hepatocytes. *J. Biol. Chem.* **265,** 12903–12909
15. Harper, M. E., and Brand, M. D. (1993) The quantitative contributions of mitochondrial proton leak and ATP turnover reactions to the changed respiration rates of hepatocytes from rats of different thyroid status. *J. Biol. Chem.* **268,** 14850–14860
16. Brand, M. D., Harper, M.-E., and Taylor, H. C. (1993) Control of the effective P/O ratio of oxidative phosphorylation in liver mitochondria and hepatocytes. *Biochem. J.* **291,** 739–748
17. Reinhart, P. H., Taylor, W. M., and Bygrave, F. L. (1982) A procedure for the rapid preparation of mitochondria from rat liver. *Biochem. J.* **204,** 731–735
18. Bhushan, A., Kupperman, J. L., Stone, J. E., Kimberly, P. J., Calman, N. S., Hacker, M. P., Birge, R. B., Tritton, T. R., and Newell, M. K. (1998) Drug resistance results in alterations in expression of immune recognition molecules and failure to express Fas (CD95). *Immunol. Cell Biol.* **76,** 350–356
19. Arceci, R. J. (1995) Mechanisms of resistance to therapy and tumor cell survival. *Curr. Opin. Hematol.* **2,** 268–274
20. Himms-Hagen, J. (1990) *Brown Adipose Tissue Thermogenesis: Role in Thermoregulation, Energy Regulation, and Obesity* (Schonbaum, E., and Lomax, P., eds) Pergamon Press, New York, NY
21. Wallace, S. (1997) *Oxidative. Stress and the Molecular Biology of Antioxidant Defenses* (Scandalios, J. G., ed) Cold Spring Harbor Laboratory Press, Cold Spring Harbor, NY
22. Skulachev, P. V. (1996) Why are mitochondria involved in apoptosis? Permeability transition pores and apoptosis as selective mechanisms to eliminate superoxide-producing mitochondria and cell. *FEBS Lett.* **397,** 7–10
23. Nishikawa, T., Edelstein, D., Du, X. L., Yamagishi, S., Matsumura, T., Kaneda, Y., Yorek, M. A., Beebe, D., Oates, P. J., Hammes, H. P., Giardino, I., and Brownlee, M. (2000) Normalizing mitochondrial superoxide production blocks three pathways of hyperglycaemic damage. *Nature (London)* **404,** 787–790
24. Voehringer, D. W., Hirschberg, D. L., Xiao, J., Lu, Q., Roederer, M., Lock, C. B., Herzenberg, L. A., Steinman, L., and Herzenberg, L. A. (2000) Gene microarray identification of redox and mitochondrial elements that control resistance to apoptosis. *Proc. Natl. Acad. Sci. USA* **97,** 2680–2685
25. Medvedev, A. V., Snedden, S. K., Raimbault, S., Ricquier, D., and Collins, S. (2001) Transcriptional regulation of the mouse uncoupling protein-2 gene. *J. Biol. Chem.* **276,** 10817–10823

Received for publication May 7, 2001.
Accepted for publication June 25, 2002.